Bulgarian Chemical Communications, Volume 48, Special Issue D (pp. 219 – 225) 2016

The size effect of titanium dioxide particles on desulfurization in a power plant

W. Cheng[1*], Y. Li[1], H.I. Schlaberg[2]

[1]*School of Energy, Power and Mechanical Engineering, North China Electric Power University, 102206 Beijing, China*
[2]*School of Control and Computer Engineering, North China Electric Power University, 102206 Beijing, China*

Received June 8, 2016, Revised September 15, 2016

To study the effect of the different states and structures of titanium dioxide on the catalytic behavior of desulfurization during a combustion process, a titanium dioxide nano-catalyst was prepared, finding that its agglomeration is serious when calcined at 100ºC. As the calcination temperature increased to 500 ºC, the agglomeration gradually weakens, and the uniformity of particles is enhanced, while remaining in the anatase structure. When the temperature was increased to 700ºC, the titanium dioxide was converted into the rutile structure, and fusion growth phenomenon occurs. Then calcium oxide desulfurization experiments with the titanium dioxide catalyst were carried out and it was found that when the calcination temperature is 500 ºC, the maximum desulfurization efficiency in the sample is achieved. Another sample became fully rutile at 900 ºC and the desulfurization efficiency began to improve.

Keywords: titanium dioxide, size effect, desulfurization, calcium oxide, burning.

AIMS AND BACKGROUND

Coal combustion processes will bring a lot of emissions, such as dust, CO_2, SO_2, NOx and heavy metals, which can cause pollution problems such as the greenhouse effect, acid rain, ozone depletion, smog and other environmental problems. Currently, these problems have raised extreme concerns at home and abroad, and the problems are so serious that they affect the human environment and need to be addressed.

For the removal of sulfur pollutants in coal-fired power plants, in general, the basic technological principles of desulfurization is that through chemical reactions between a desulfurization agent and the emissions, the gaseous emissions are solidified into a reaction product of solid state, so as to achieve the elimination of the polluting emissions. In this case, whether the desulfurization agent is renewable or not, has a relationship with the running costs of the system and waste of land resources and secondary pollution of the environment.

The TiO_2 catalytic action stems mainly from the transition metal characteristics of titanium. Under different reaction conditions, it directly affects the reaction substance or indirectly affects the reaction process. The bond energy of Ti and the corresponding ligands are weak, and the catalytic action tends to be of an ionic character. As a new environmentally -friendly material and being non-toxic and harmless, it has garnered much attention in recent years due to its many excellent properties and can be used as a catalyst or carrier in many of these reactions. The preparation method, application and development of TiO_2 materials have become one of the main points of its study [1].

Ruan et al. [2] investigated an industrial honeycomb catalyst in a power plant, adding different amounts of arsenic in the catalyst to study the performance effects of arsenic on a commercial V_2O_5-WO_3 / TiO_2 catalyst. A remarkable effect on the activity of the catalyst was observed. Only a little arsenic can result in the decrease of the catalyst activity. When As / V is 0.2, the activity of the initial 92.02 percent is down to about 74%. When increasing the catalyst, its activity declined. Arsenic majorly impacted VOx species on the catalyst surface, and made the vanadium species diverse, but did not affect the chemical character of V_2O_5/ TiO_2. It has a certain influence on the acidic sites of the catalyst surface, reducing Bronsted acid sites of the adsorbed NH_3.

The Hg oxidation activities of several commercial V_2O_5/WO_3 (MoO_3)/TiO_2 honeycomb and plate type DeNOx catalysts were identified for the DeNOx inactive case and compared with their DeNOx activities [3]. In this way, it was possible to show that the velocities of Hg oxidation and DeNOx reactions are of the same order of magnitude. The DeNOx-active state of the catalysts had a strongly negative impact on the oxidation of elemental Hg that could not be explained solely by an inhibition effect of ammonia. Under these conditions, even reduction of oxidized Hg occurred on the catalyst. Our understanding of the control variables for Hg oxidation in SCR DeNOx plants has to be amended in light of these slowing effects

* To whom all correspondence should be sent:
E-mail: cwl@ncepu.edu.cn

and has to take the induced reduction into account.

Xi, et al. [4] have investigated a composite SCR carrier prepared with 10% cordierite and titanium dioxide. And it did not become rutile when calcined at 600℃, meanwhile samples of V_2O_5 and WO_3 crystal diffraction peaks did not appear. The catalyst wear rate, water absorption and shrinkage rate is not heavy, avoiding cracking of the honeycomb catalyst in the heat treatment to improve the thermal stabilization. In the experiments, the reaction temperature ranges between 250 - 460℃, the denitration rate is more than 80%. Hg^0 oxidation by chlorine over CeO_2–TiO_2 catalysts with different CeO_2/TiO_2 ratios was investigated both in the absence and the presence of SO_2 [5]. An addition of SO_2 did not inhibit the adsorption of HCl on pure CeO_2; however, it inhibited reactions between Hg^0 and chlorine species over pure CeO_2, hence resulting in a decrease of Hg^0 oxidation efficiency. The desulfurization ability of CaO–Al_2O_3–SiO_2–TiO_2 slag at 1 873 K was studied through a slag-metal desulfurization experiment [6]. The experimental indices considered were the sulfur distribution coefficient of the slag and the desulphurization ratio. The effect of the mass percentage of Al_2O_3 and TiO_2 is significant. Under optimal experimental conditions, the slag system with TiO_2 can meet the desulfurization requirements of steelmaking, which is a good way for resource utilization of solid waste containing titanium. The oxidative desulfurization of several sulfur compounds with a mixture of hydrogen peroxide and formic acid was studied [7]. The catalytic activity of a nanocomposite was tested on oxidative desulfurization of actual gas oil and results are compared with that of model sulfur compounds. This Keggin-type supported catalyst was shown to be able to have oxidative desulfurization of model sulfur compounds and actual gas oil with a high yield.

As a typical photocatalytic material, titanium dioxide has been applied extensively in technical applications. In recent years, some scholars have reported research developments in titanium dioxide used in desulfurization.

Zhao et al [8,9] studied experimentally supported TiO_2 photocatalysts in simultaneous desulfurization and denitrification in flue gas. Increasing removal efficiency by aerobic participation; the NO removal efficiency increased when the water vapor content was increased to a certain extent. When the exposure time is maintained for 100 min, the optimum SO_2 and NO removal efficiency is obtained. The concentration of sulfate and sulfite in the removal process increased with the increase of the initial concentration, and the removal product SO_4^{2-} is the dominant species. When the SO_2 concentration is low, the oxidation action is dominant. But with the concentration going up, the oxidation advantages are weakened and the dissolving and absorption abilities are enhanced.

A TiO_2-aluminum silicate fiber nanocomposite, synthesized by a sol–gel method, is proposed to be used as a photocatalyst for the removal of multiple pollutants of SO_2, NO and Hg^0 in a simulated coal combustion flue gas [10]. The TiO_2-aluminum silicate fiber calcined at 500℃ exhibited the biggest BET surface area and highest photocatalytic activity. In experiments, the removal efficiencies for SO_2, NO and Hg^0 at 120℃ and with a UV intensity of 3 $mWcm^{-2}$ can reach 33%, 31% and 80% respectively. However, the addition of water vapor to the simulated flue gas inhibited the oxidation of SO_2, NO and Hg^0. The UV intensity was the most important factor in the photocatalytic oxidation.

Han et al. [11] prepared a nano- TiO_2 composite photocatalyst supported by activated carbon fibers, and carried out research by simultaneously removing high concentrations of sulfur dioxide and nitric oxide under ultraviolet and visible light conditions. Under visible light conditions, SO_2 and NO removal efficiency were higher. The TiO_2 photocatalytic action is dominant in the desulfurization and denitrification process.

Titanium dioxide supported by multi-walled carbon nanotubes (MWCNTs/TiO_2), and Cu doped TiO_2 supported by MWCNTs (MWCNTs/Cu-TiO_2) were synthesized via a sol–gel method [12]. The oxidation and removal efficiencies of SO_2 and NO in a simulated flue gas were investigated experimentally in a fixed-bed reactor. The optimal conditions (73 mg/m^3 NO, 155 mg/m^3 SO_2, 8% O_2, 5% H_2O) were determined, and 62% and 43% of total SO2 and NO removal were achieved on 15% MWCNTs/Cu–TiO_2. The integrated desulfurization and denitration efficiencies were lower than that in the baseline experiments due to SO_2 and NO competing for adsorption sites.

Wang et al [13] have compared the impact of nano-titanium dioxide on the desulfurization during the combustion in two kinds of coals. The desulfurization performance in the coal combustion of nano- TiO_2 and CaO changes the microstructure of ash, the ash loses pores, the CaO lattice structure which makes the CaO aperture larger, increases the number of pores and the specific surface, improving the CaO sintering characteristics that promote SO_2 and CaO becoming calcium sulfate. Nano- TiO_2 has some adaptability for different

coals, especially high-sulfur coal. The optimal reaction conditions for nano- TiO_2 are a dosage of 8% TiO_2 nanoparticles, Ca / S molar ratio of 2, a combustion temperature of 850°C in the desulfurization experiments. Nanosized titanium oxide powder was prepared via the sol-gel process [14]. The calorific value of the coal and the fusion temperature of the coal ash were lowered by adding CaO, while on the other hand adding nano-TiO_2 to coal effectively increased the calorific value and the melting temperature. Meanwhile, the coal combustion efficiency and desulfurization in the combustion could be effectively improved by the co-action of TiO_2.

Photocatalysts with different mass ratios of TiO_2/g-C_3N_4 were prepared by a two-step method [15]. The photocatalytic oxidation activity of the samples was evaluated by photooxidation of dibenzothiophene. Reaction conditions, such as the amount of H_2O_2 andTiO_2 loading, were investigated in detail. The results showed that the removal of dibenzothiophene could get to 98.9% under optimized conditions after 2 h at room temperature. The oxidation reactivity of the different sulfur compounds was found to be in the order of dibenzothiophene > benzothiophene > n-dodecanethiol (RSH). Further studies showed that dibenzothiophene and its derivatives were converted to the corresponding sulfone, which could be extracted by a polar solvent. The catalytic activity of titanate nanotubes in the oxidation of dibenzothiophene by using H_2O_2 was investigated [16]. Titanate nanotubes were synthesized by alkaline hydrothermal treatment of anatase TiO_2 followed by washing either with water to produce titanates with high sodium content or with aqueous HCl to obtain protonated titanates. These results were correlated with the production of reactive radicals as observed by electron paramagnetic resonance and with dibenzothiophene adsorption capacity. Favorable reaction conditions were found to be low temperatures (25°C) and H_2O_2/ dibenzothiophene = 4. Reactions at elevated temperatures and H_2O_2 concentrations lead to significant reduction in catalyst activity, associated with partial phase transformation and premature deactivation of the catalytic sites. A.H.M. Silver supported on mixed oxides Ag/TiO_2–Al_2O_3 shows promise as an advanced organosulfur adsorbent with deep desulfurizing ability and scalability to be fitted into on-board fuel cell systems [17]. This paper presents the performance, characterization, and desulfurization mechanism of Ag/TiO_2–Al_2O_3 adsorbent for applications in pre-reformate cleaning of Proton Exchange Membrane fuel cells. Anatase-TiO_2 dispersion on Al_2O_3 provided increased adsorbent activity, higher surface acidity and exerted in more defect sites for Ag incorporation. TiO_2–Al_2O_3 provided both strong and weak Bronsted sites.

By using two specific titanium dioxide materials, such as the anatase of 5,10,50 nm and rutile mine of 10 × 40, 30 × 40, the experiments were carried out to obtain the features of titanium dioxide nano-materials on deposition and aggregation in sodium chloride aqueous solution[18]. The stability between 10 × 40 rutile and 50 nm anatase at pH = 7 is the best, but the morphology and the chemical structure is not related to this. And impurities in raw materials such as silicon and phosphorus components have something to do with the surface charge. In the aggregation experiment, the critical concentration of 50nm anatase material is the highest, followed by 10 × 40 rutile and 5nm anatase.

Roncaroli et al. [19] studied two different titanium dioxide samples. It showed that their equilibrium properties are relatively similar, and the influence of the particle size and specific surface area on the adsorption rate is large in the dynamics of titanium dioxide thin films. That is why the internal diffusion capacity, in which the finer the particles are, the higher the porosity is. Dittmann et al. [20] found that very fine particles may be solidified into a dense ceramic material at low temperatures in a sintering process when grain growth and pore generation are avoided. During the sintering of titanium dioxide nanoparticles by adding elemental chlorine, the influence of phase transformation, the thickening rate and particle growth are considered. It was found that at 900 degrees, the doped chlorine leads to strong particle growth, but the thickening rate and phase transition temperatures are low, and the final density decreased by 1.5 %.

Gondek et al. [21] using the sol - gel and pull coating method, prepared a TiO_2 film attached to a sodium calcium glass lining, discovering the size effect. For a comparative analysis of TiO_2 films and TiO_2 films with an intermediate silica oxide layer, and the width of the energy gap and the Urbach energy were measured, resulting in the energy gap in the range of TiO_2 the film thickness between the glass substrate and the TiO2 thin film, which was caused by sodium ions. The impact of silicon ions on the direct energy gap was found in the TiO_2 film adhered to a soda-lime glass substrate with pre-coated SiO_2 layer.

Due to the advantages of TiO_2 materials such as being non-toxic, cheap, efficient, non-corrosive and

so on, TiO_2 is widely used as a catalyst or catalyst carrier in the preparation of adsorbents or catalysts in desulfurization and denitrification. Obviously, different sizes of TiO_2 will have different impacts on the catalytic efficiency of desulfurization and denitration, so different sizes of TiO_2 have great significance for desulfurization and denitration.

In this paper, titanium dioxide of several sizes were prepared by hydrolysis of titanium grease, and the size effects of experimental desulfurization were studied on the basis of systematic characterization of titanium dioxide.

EXPERIMENTAL

Titanium dioxide nanopowders were prepared by the sol - gel method, using tetrabutyl titanate and deionized water as raw materials. Tetrabutyl titanate with deionized water at a volume ratio of 1:2. A beaker with 300 ml of deionized water was placed in an electric mixer.The mixer was adjusted to a certain speed, and then 150 ml of tetrabutyl titanate was added dropwise into deionized water while continuously being stirred. After continuous stirring for 6h, the solution was placed in the shade and left standing for 24h. The mixture was then dried to get a solid yellow powder. The powder was divided into five equal parts, respectively calcinated in a muffle furnace at 100, 300, 500, 700 and 900ºC for 4h. This made a series of nano-sized titanium dioxide powders. The samples were defined as Sample 1, Sample 2, Sample 3, Sample 4 and Sample 5 by the calcination temperature.

The experimental combustion desulfurization system is shown in Figure1. Firstly, lignite coal and titanium dioxide nano-powder sample were mixed, and put into a porcelain boat which can be taken into the tube furnace. This is then connected to an absorption bottle, introducing oxygen. Secondly, the samples were preheated to 500 ºC for 5 min to discharge volatiles and prevent coal deflagration, then further heated to a specified combustion temperature, combusting takes place for 25min using pure oxygen, and the SO_2 of the exhaust gas is absorbed by a lime solution. Finally, the SO_2 content of the flue gas was measured by adding iodine liquid which has the effect of desulfurization. For subsequent samples 2 to 5, the same experimental desulfurization methods were applied.

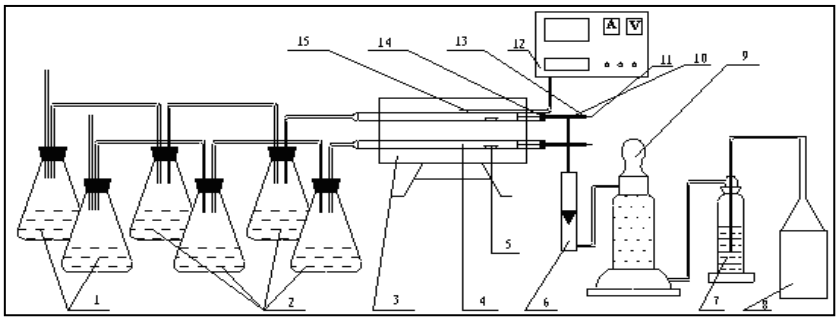

Fig. 1. Burner gas desulfurization experimental apparatus. 1 lime solution; 2 absorption bottle; 3 tube furnace; 4 burner tube; 5 porcelain boat; 6 meter; 7 scrubber; 8 storage cylinder; 9 drying tower; 10. T -tube; 11 push rod; 12 temperature controller; 13 turn plastic cap; 14 rubber stopper; 15 thermocouples.

RESULTS AND DISCUSSION

Changes in the structure of titanium dioxide

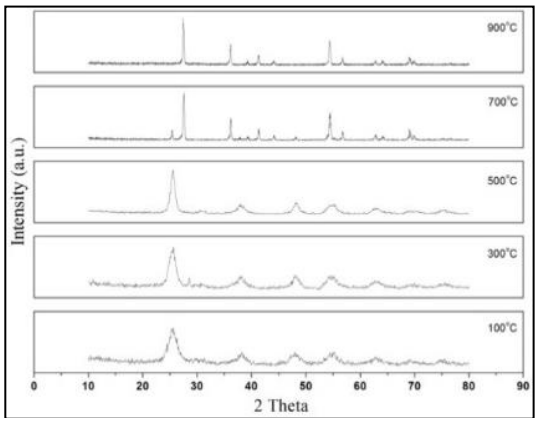

Fig. 2. XRD titania obtained at different temperature.

X -ray diffraction (XRD) pattern analysis can be used to find variation of the size and configuration, a case is shown in Figure2. As can be seen, at a temperature of 100ºC, 300ºC, 500ºC, a series of peaks in the diffraction pattern are consistent with anatase titanium dioxide, and showed that the obtained crystalline powder has the anatase structure. In addition, the half-width of the diffraction peaks of the sample 1, 2, and 3 are wider than sample 4 and 5, and show that the particles sizes of the three powders are small. As the temperature increases, the diffraction peaks gradually sharpened. When the temperature exceeds to 500ºC, the diffraction peaks of sample4 are obviously refined at 700ºC. When the peaks increase, the powder particle size becomes large, and at that time the structural phase transition

appears. Comparing with the standard rutile Atlas, each peak corresponds with titanium dioxide rutile. Through the above analysis, it is easy to find that for the samples in the range of 500-700ºC an obvious structural phase transition occurs, namely, the structure transition from anatase to rutile happens.

To further carry out the quantitative analysis of the phase change process, Figure 3 shows the description of the rutile phase transition rule with a phase transformation. In Figure 3 using the following formula is used to calculate the phase variables:

Variable phase (%) = Σ rutile peak / (Σrutilepeak + Σ anatase peak rutile peak) (1)

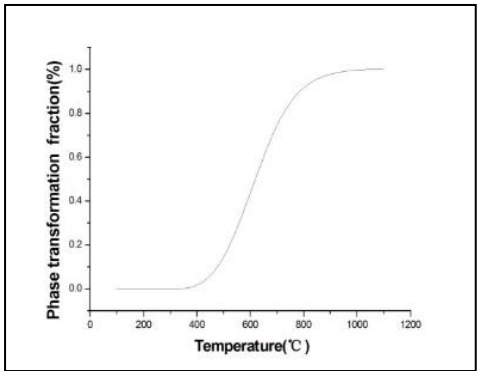

Fig. 3. The different temperatures to obtain titania phase transition diagram.

Size effect of titanium dioxide

A scanning electron microscope (SEM) was used to study the change mechanism of the particle size in calcined titanium dioxide at different temperatures, discussing the phenomenon of agglomeration and fusion grown in the process. The size effect refers to the fact that the reaction efficiency of desulfurization and denitrification can be improved after the character of the particle changes because agglomeration and fusion changes the size of the particle. The size effect is not an effect due to the original particle size but rather due to the grain size after undergoing a calcination process at different temperatures. In Figure4, SEM pictures of titanium dioxide particles of (a), (b), (c), (d) and (e) correspond to calcination temperatures of 100, 300, 500, 700, 900 ºC respectively. From the SEM scanning, it can be seen that the calcination temperature has a great influence on the particle size of titanium dioxide. Figure4(a) clearly shows that at a calcination temperature of 100℃, the particle size is about 1.3540μm, while the grain size of the titanium dioxide in the sample is typically 6 nm. Thus, the agglomeration of titanium particles at this time is quite serious.

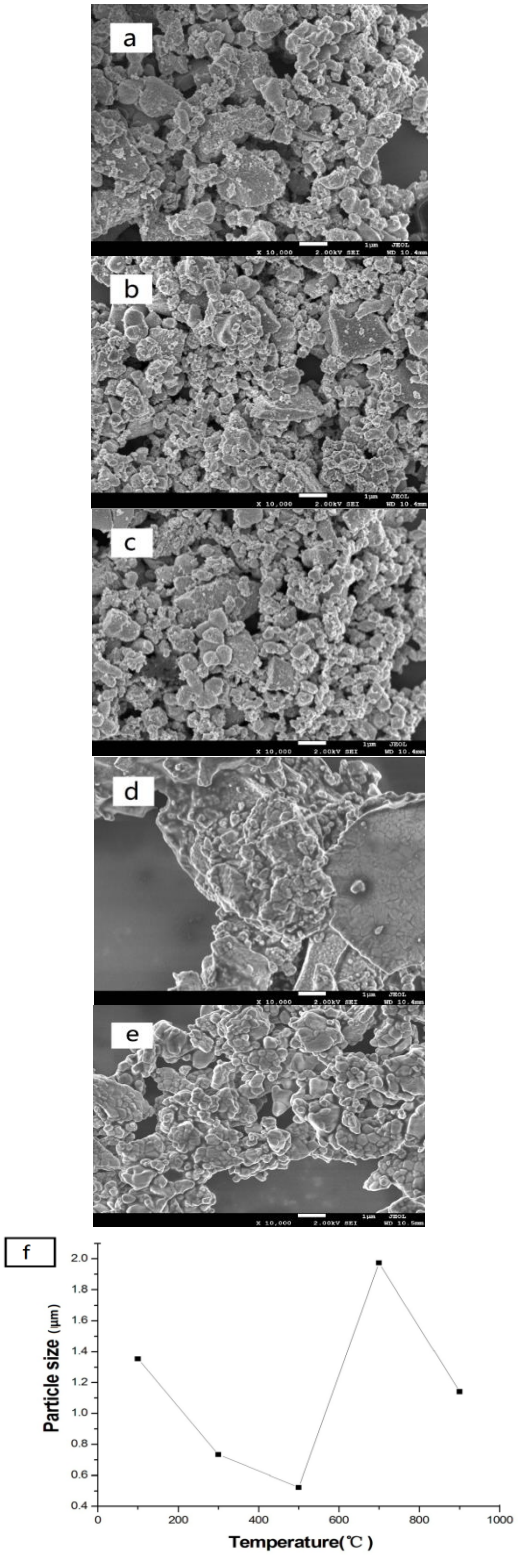

Fig. 4. Titanium images and synthetic curves at different temperatures:

(a)calcining temperature 100℃;
(b) calcining temperature 300℃;
(c) calcining temperature of 500℃;
(d) calcining temperature 700℃;
(e) calcining temperature 900℃;
(f) grain size versus temperature.

When the calcination temperature is 300℃, Figure 4b shows that the agglomeration of titanium dioxide grain at this time has been reduced compared to Figure 4a, but there still is agglomeration of large pieces of particles. When the calcination temperature is 500ºC, Figure 4c, shows a change of the titanium dioxide particles which are now relatively small and uniform, while the specific surface area is still relatively large. At 700 ºC as shown in Figure 4d, the fusion growth phenomenon of titanium dioxide particles appears, this being different from Figure 4a and Figure 4b where the agglomeration of titanium dioxide takes place. When the calcination temperature is 900 ºC, Figure 4e, the grain growth phenomenon of titanium dioxide particles is quite obvious and cracking occurs, the grain growth size of the particles is significantly less than that at 700 ºC. Figure 4f describes the curves that the particle size of titanium dioxide with calcination temperature. Observed at 500ºC, the titanium dioxide particles are smallest, while the biggest are found at 700 ºC.

Desulfurization effect analysis

Each of the five samples which had 8% calcium oxide was mixed with pulverized coal, then the experiments of desulfurization during combustion were carried out. The experimental data can be described as a curve which shows the relation between the different samples and the desulfurization efficiency, as shown in Figure5. The desulfurization efficiency is related to the calcination temperature of the titanium dioxide sample. The curve rises in the beginning, then falls, and finally rises. The Desulfurization efficiency of sample 1 was low, and desulfurization efficiency of samples 2 to 3 gradually increased. Sample 3 was prepared at 500ºC, and its desulfurization efficiency was the highest. The desulfurization efficiency of sample 4 is lower. With the experiment of sample 5, the desulfurization efficiency increased again.

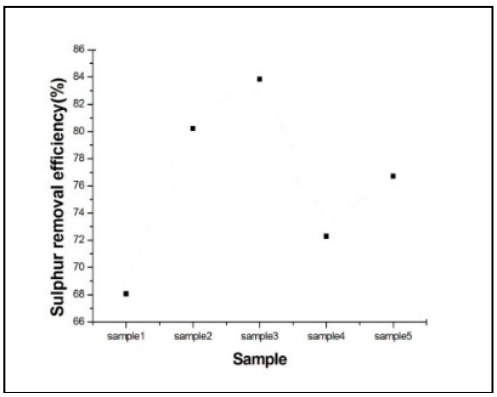

Fig. 5. Desulfurization efficiency varies with different samples of the curve.

The differences of particle size of titanium dioxide in the reaction are large, which represents different effects. Under normal ambient conditions, the crystal size of a titanium sample is about 6nm. However under other special physical and chemical conditions, the group size of some particles will multiply thousands of times, then the physical and chemical influences are not same. When the micelle size of a titanium dioxide particle is under certain range, the size effect will happen [18], at that time, the electronic energy levels near the Fermi level range from quasi-continuous to discrete, as the energy gap becomes wider. When the difference of the energy level is bigger than that of heat, light, electromagnetic energy, it results in a significant difference in the characteristics of the nanoparticle's magnetic, optical, acoustic, thermal, electrical, superconducting properties. Moreover, from the point of view of the crystal structure of titanium dioxide, the chemical composition of anatase and rutile ore are formed by titanium dioxide, and both ores are tetragonal, but their arrangement and connections are different. In Figure 6, each of the octahedral are connected with ten surrounding octahedral in the rutile crystal, wherein there are two shared edges and eight shared vertices. In the anatase crystal, each is connected with the surrounding eight octahedral, wherein there are four shared edges and four shared vertices. In contrast, the anatase crystal structure is more open than the rutile structure, so the catalytic activity of anatase is relatively stronger than rutile.

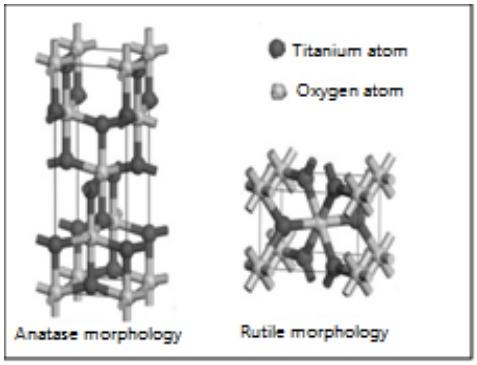

Fig. 6. Molecular structure of anatase and rutile titanium mine.

In the sample preparation process, when the calcination temperature is increased from 100ºC to 500ºC, the agglomeration of titanium dioxide gradually decreases, the specific surface area increases, and the adsorption capacity increases, at this stage the particle sizes are relatively small. In the coal combustion experiment when mixed with both calcium oxide and the titanium sample, in the beginning, the desulfurization efficiency gradually

improves, at this stage, it is all in the anatase state. When the experiment is in the temperature interval between 500ºC and 700ºC, the anatase structure gradually transforms to the rutile structure, at the same time the desulfurization efficiency begins to decline gradually. After the temperature reaches 700ºC, the anatase structure completely transforms to the single-phase rutile structure, at this time the dioxide particles of the fusion growth start cracking, resulting in the particle size becoming smaller, and the adsorption capacity of sample 5 rises.

In summary, for titanium dioxide sample 3, the agglomeration phenomenon is very weak, the size is small, the specific surface is large, and the adsorption ability is stronger, but the opposite happens in the case of anatase.

CONCLUSIONS

When the nano- titanium oxide catalyst was prepared at calcination temperatures from 100ºC to 500ºC, the phenomenon of agglomeration appeared, the resulting particles had an anatase structure. In the calcination temperature range of 500ºC-700ºC, the anatase structure significantly transforms to rutile, and the fusion growth phenomenon occurs. After the calcination temperature reaches 700ºC, the structure is completely in the rutile state, cracking of the fusion growth particles appears and the particle size becomes smaller.

In the coal combustion experiments with titanium dioxide and calcium oxide, the size effect of titanium dioxide on desulfurization is very obvious. No matter whether TiO_2 is in either the anatase or rutile state, the agglomeration and fusion growth phenomenon influences the desulfurization because of the particle size change. The particles of sample 1 are fairly small, thus agglomeration is serious and desulfurization efficiency is not high. For sample 2 and sample 3, the desulfurization efficiency gradually increases. For the samples 4 and 5 which completely converted to the rutile structure, the desulfurization efficiency decreases and then rises.

Acknowledgements: *This work was supported by Beijing Natural Science Foundation (No.3132017), and National Natural Science Foundation of China (No. 51476056).*

REFERENCES

1. J.W. Xu, L.Y. Wang, S.H. Chen, Y. Pang, *Mod. Chem. Ind.*, **31**, 21(2011).
2. D.L. Ruan, S.W. Pan, Z.L. Wei, B.C. Huang, H. Cheng, *Chem. Ind. and Eng. Prog.*, **33**, 925 (2014).
3. R. Stollea, H. Koesera, H. Gutberletb, *App. Cata. B: Environ.*, **144**, 486 (2014).
4. W.C. Xi, Q.C. Liu, *Chin. J. Environ. Eng.*,**7**, 2262 (2013).
5. H.L. Li, C.Y. Wu, L.Q. Li, *Fuel*, **113**, 726 (2013).
6. K. Dong, L. Wu, W.J. Liu, R. Zhu, *Iron Steel Inst. Japan International*, **54**, 2248 (2014).
7. A.F. Shojaei, M.A. Rezvani, M.H. *Fuel Process. Technol.*, **118**, 1 (2014).
8. Y. Zhao, J. Han, *J. Power Eng.*, **27**, 411 (2007).
9. Y. Zhao, L. Zhao, J. Han, *Proceedings of the CSEE*, **27**,51 (2007).
10. Y. Yuan, J.Y. Zhang, H.L. Li, *Chem. Eng. J.*, **192**, 21 (2012).
11. J. Han,Y. Zhao, ,*Environ. Sci.*, **30**, 997 (2009).
12. H. Liu, X.Q. Yu, H.M. Yang, *Chem. Eng. J.*, **243**, 465 (2014).
13. S.Q. Wang, C.R. Su,Y. Zhao, *J. North China Elec. Pow. Univ.*, **38**,89 (2011).
14. Y. Zhao, S.Q. Wang, Y.M. Shen,X.J. Lu, *Energy*, **56**, 25 (2013).
15. C. Wang, W.S. Zhu, Y.H. Xia, H. Xia, *Ceram. Int.*, **40**, 11627 (2014).
16. E. Lorencon, D.C.B. Alves, K. Kramvrock, E.S. Avila, *Fuel*, **132**, 53 (2014).
17. A.H.M. Shahadat Hussain, B.J. Tatarchuk, *Fuel Process. Technol.*, **126**, 233 (2014).
18. X.Y. Liu, G.X. Chen, C.M. Su, *J. Colloid. Interf. Sci.*, **363**, 84 (2011).
19. F. Roncaroli, M.A. Blesa, *J. Colloed. Inerf. Sci.*, **356**, 227 (2011).
20. R. Dittmann, E. Wintermantel, T. Graule, *J. Eur. Ceram. Soc.*, **33**, 3257 (2013).
21. E. Gonded, P. Karasinski, S. Drewniak, *Phys. E: Low-dimen. Sys. Nanostr.*, **62**, 128 (2014).